

TURBULENT MIXING VIA EDDIES GENERATION IN PULSATING FLOW MODE

O.A. Azarova* and Yu. F. Kolesnichenko**

* Computing Center of RAS

olga_azarova@list.ru

** Institute of High Temperatures RAS

kolesnichenko@ihed.ras.ru

Key words: *thin rarefied channel - shock layer interaction, system of Euler equations, contact discontinuity instability, pulsating flow, turbulent mixing, separation area.*

1. STATEMENT OF THE PROBLEM

Global flow reconstruction as an effect of thermal non-homogeneities in supersonic flow was widely investigated. The investigations on interaction of heat releases with shock layers^{1,2} are the preliminaries of this work regarding some flow reconstruction effects established. Possible accompanied phenomena are pulsating flow modes establishing, generation of instabilities of the boundaries between hot and cold gases and their turbulent mixing²⁻⁶.

In this work the results of numerical modeling of the pulsating flow with contact discontinuities instabilities like Richtmyer-Meshkov and shear-layer instabilities are presented. Thin infinite rarefied channel energy release – cylinder shock layer interaction is considered. In^{2, 7-11} the similar statement of the problem was used for plane and cylinder flow symmetry. Numerical modeling is based on the Euler equations in the divergence form for ideal gas:

$$\frac{\partial \bar{U}r}{\partial t} + \frac{\partial \bar{F}r}{\partial x} + \frac{\partial \bar{G}r}{\partial r} = \bar{H},$$

$$\bar{U} = \begin{pmatrix} \rho \\ \rho u \\ \rho v \\ E_s \end{pmatrix}, \bar{F} = \begin{pmatrix} \rho u \\ p + \rho u^2 \\ \rho uv \\ u(E_s + p) \end{pmatrix}, \bar{G} = \begin{pmatrix} \rho v \\ \rho uv \\ p + \rho v^2 \\ v(E_s + p) \end{pmatrix}, \bar{H} = \begin{pmatrix} 0 \\ 0 \\ p \\ 0 \end{pmatrix}.$$

Here ρ , p – density and pressure of the gas, u , v – x - and r - components of the gas velocity, $E_s = \rho(\epsilon + 0.5(u^2 + v^2))$, ϵ - specific internal energy, the ratio of specific heats $\gamma = 1.4$. The non-dimensional variables are used. The unit of length measure is $l_n = 10^{-2}$ m the time and velocity units of measure are, respectively, $t_n = 1.6 \times 10^{-5}$ s and $u_n = 6.27 \times 10^2$ m/s. Initial flow parameters corresponded to the normal conditions were $\rho_0 = 1$, $p_0 = 0.2$, $u_0 = 1$, $v_0 = 0$, Mach number of oncoming flow was 1.89. On the entrance boundary the parameters of oncoming flow were used. The boundary conditions had a sense of reflection on the x -axis and on the body's boundaries, and of absence of the reflection on the exit boundaries.

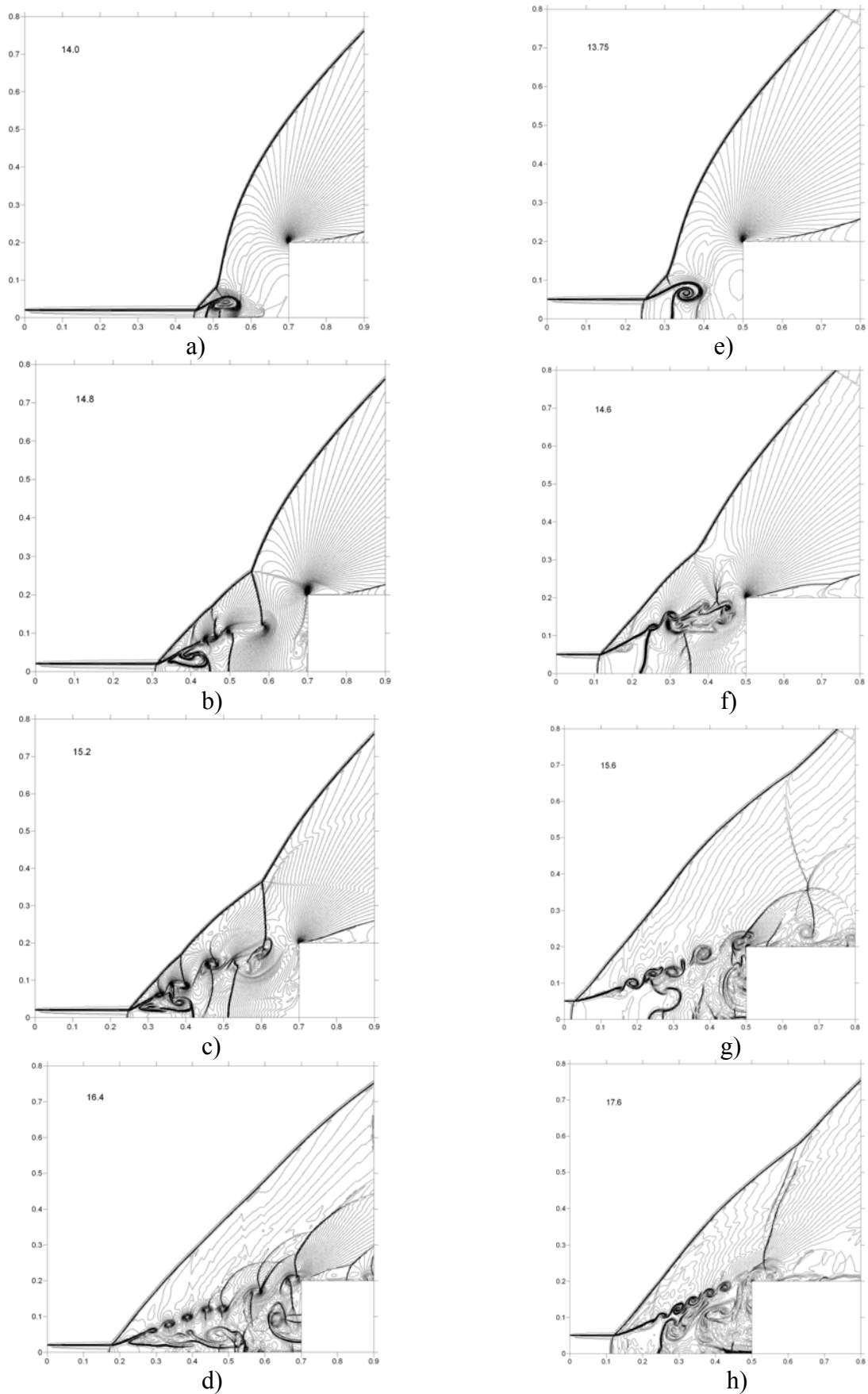


Fig.1. Dynamics of the processes in isochors for $d=0.1$, (a) - (d), and $d=0.25$, (e) - (h).

An energy release regarding as an infinite rarefied channel is assumed to arise instantly in the steady flow in front of the bow shock wave at the time moment t_i . The energy release was modeled via the entrance boundary conditions ($x=0$) as an infinite channel of low density ρ_i , $\rho_i=\alpha_p\rho_0$ for $0\leq r\leq R$, where R is the channel radius, ρ_0 is the density in undisturbed flow, α_p - the degree of gas rarefaction in the channel. Other parameters were equal to those of undisturbed flow. Thus the boundary condition on the entrance boundary was:

$$\rho(0,r,t)=\rho_0, p(0,r,t)=p_0, u(0,r,t)=u_0, v(0,r,t)=v_0 \text{ for } r\geq 0 \text{ and } t<t_i,$$

$$\rho(0,r,t)=\rho_i=\alpha_p\rho_0, p(0,r,t)=p_0, u(0,r,t)=u_0, v(0,r,t)=v_0 \text{ for } 0\leq r\leq R \text{ and } t\geq t_i.$$

In these calculations $d=R/R_b=0.1/0.25$ (R_b is the body radius), $\alpha_p=0.5$, $t_i=13.01$.

The method employed is the original cylinder two-dimensional analog of the difference scheme¹² on a minimal stencil. The scheme is conservative and has the second order of approximation in space and in time. The boundary conditions were expressed via flux functions and included to the calculations without breaking the conservation laws in the calculation area. The grid (1600×1600) and the space steps values equal to 0.0005 were used.

2. CALCULATION RESULTS

1. Generation and distortion of Richtmyer-Meshkov instability; generation of shear-layer instabilities; heated channel formation.

Blunt cylinder AD body is considered; radius of the body R_b is equal to 0.2. The energy release is assumed to be an infinite cylinder of constant density. Flow isochors for the interaction of the low density channel with the shock layer for $d=0.1$ (left side) and $d=0.25$ (right side) are presented in Fig.1. The values of time moments are defined in the upper left corner of the slides. The beginning of the interaction process is connected with the bow shock wave motion from the body and generation of contact discontinuity instability like Richtmyer-Meshkov instability⁴ (Fig.1a, 1e). The reason of the instability generation is the impulse effect of the bow shock wave upon the contact discontinuities (horizontal and vertical) representing the boundaries of the rarefied channel. In the case of $d=0.1$ the heated area expanding in the direction to the body is obtained (Fig.1b). For $d=0.25$ this phenomenon doesn't take place (Fig.1f). This phenomenon was registered for the spherical shock layer – elongated thin energy source interaction⁶, too. Thus, this phenomenon is inherent to different types of energy releases with the shape of thin rarefied channels and for different flow symmetry. It is seen that for $d=0.1$ the shocks included into the triple configuration generating in the point of the bow shock wave fracture are more strong than for $d=0.25$ (Fig.1b, 1c and 1f). New boundary instability generation is seen in Fig.1b, 1f. This instability is shear-layer instability; it is initiated by triple point configuration – contact discontinuity interaction¹¹.

The next stage of the process is connected with oscillations of the bow shock, irregular shear-layer instabilities generation and heated channel formation inside the shock layer in the case of $d=0.1$ (Fig.1d, 1h). The process of shear-layer instabilities generation is similar for all kinds of channels. Vortex structure generated from the rolled contact

boundaries reaches the body, decreasing the pressure on it and as the result some time later the bow shock is broken. The pressure near the body continues to fall down causing return motion of the bow shock wave. Near the front surface of the body the reversal circulation flow is forming caused the pulsations of the flow. Mechanism of the flow pulsations is established to base on relationship between circulation and reversal flows and presence or absent of the flow from the heated area¹¹. At the end of this stage the bow shock front becomes nearly flat and the eddies form in a line. Stochastic eddies form the flow separation area of turbulent-like fluctuations adjacent to the body's surface.

2. Separate vortices centers trajectories consideration: two different types of vortex behavior.

The trajectory analysis has been conducted. The separate vortex center trajectory $\mathcal{L}(X_v, Y_v)$ was considered. It was defined in parametrical form by the relations:

$$\frac{dX_v}{dt} = u_v, \frac{dY_v}{dt} = v_v,$$

where X_v, Y_v, u_v, v_v – the values of coordinates and velocity projections of the vortex center. It is established that there are possible two types of the vortex dynamics. In one case when the flow from the heated area is taken place the vortices are blown away along the body from the calculation area. In the second case when the flow from the heated area is locked the vortices return to the separation area producing turbulent-like medium non-homogeneities. Dynamics of vortex center coordinates X_v, Y_v and pressure value in the vortex center P_v for these two different types of vortex behavior is presented in Fig.2. The according dynamics of the bow shock wave coordinate X_w is presented, too.

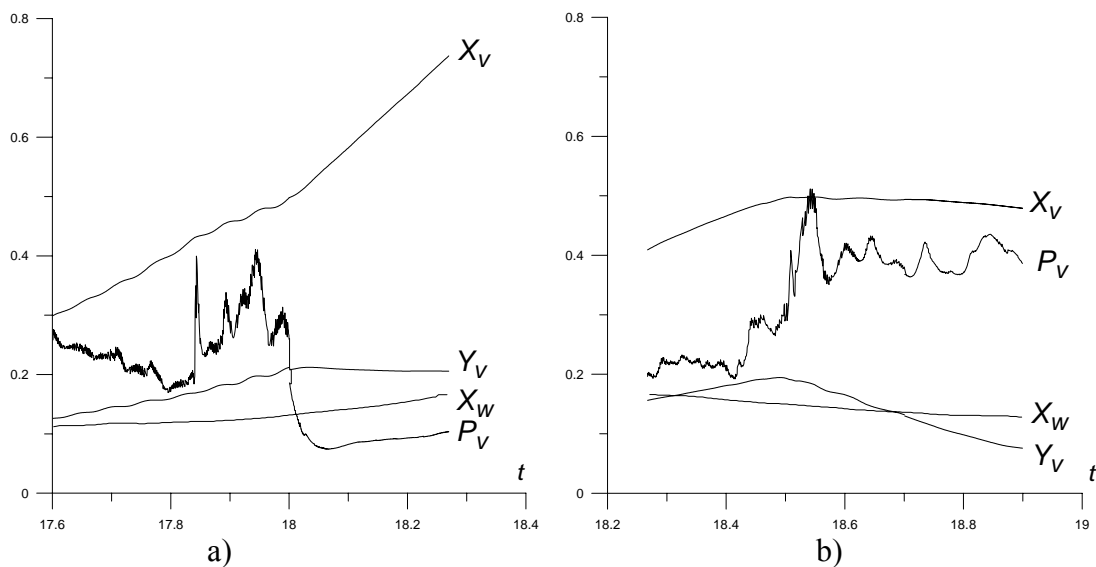


Fig.2. History in time of vortex center coordinates X_v, Y_v , pressure in the vortex center P_v , and the bow shock coordinate X_w ($d=0.25$): a) – the case of the vortex leaving the calculation area; b) – the case of the vortex returning to flow separation area.

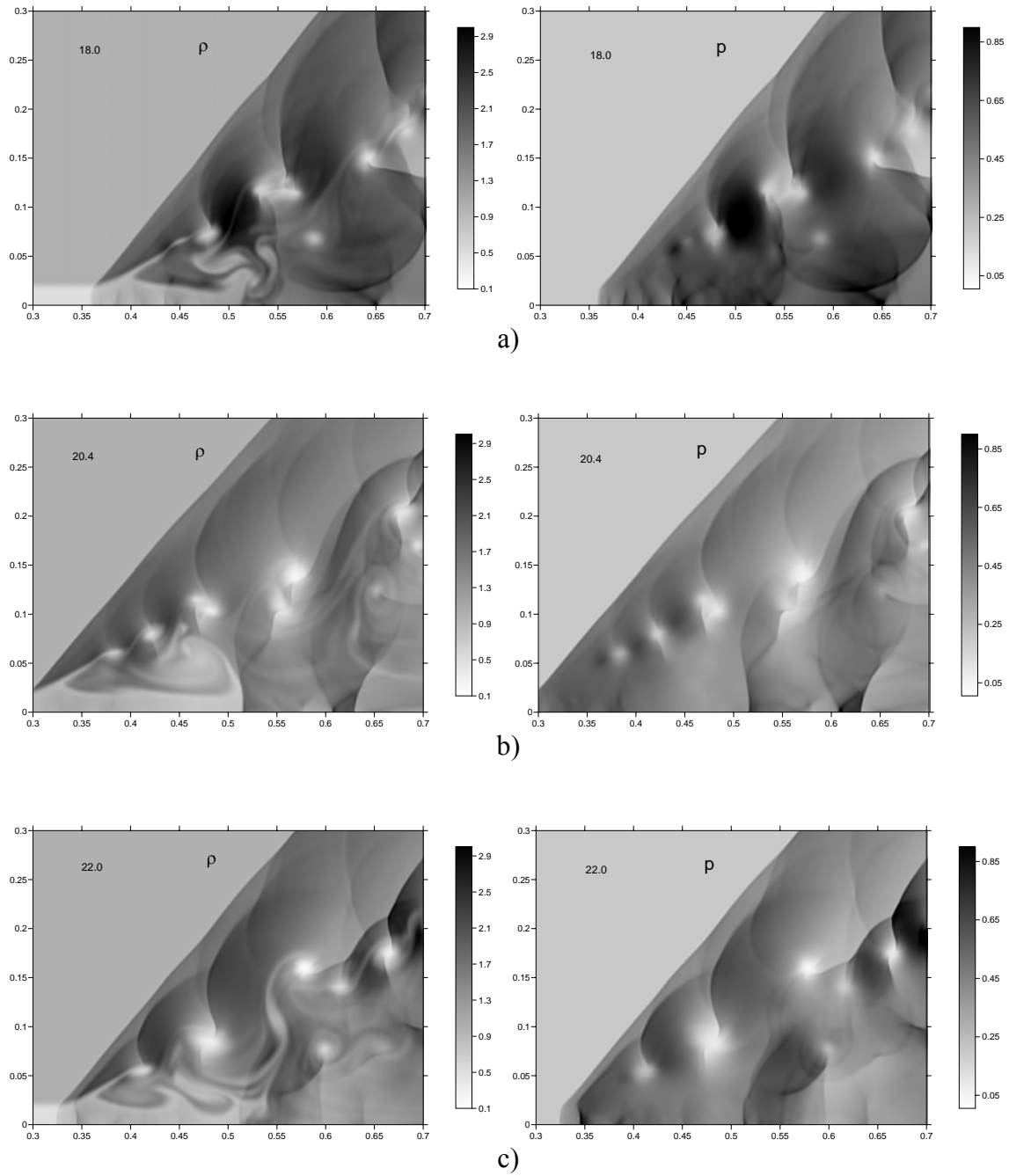


Fig.3. Fields of density and pressure, $d=0.1$: increasing of turbulent mixing inside the separation area, a) $t=18.0$, c) $t=22.0$; decreasing of turbulent mixing, b) $t=20.4$.

3. Turbulization of the separation area and turbulent mixing of hot and cold gas layers via eddies generation.

In the case of $d=0.1$ the eddies are stronger than for $d=0.25$. Thus, the turbulization is stronger, too, and the strength of the reversal eddies is turned out to be sufficient to provide turbulent mixing of the hot gas in the formed channel and cold surrounding gas inside the separation area. The fields of the flow parameters for turbulent mixing inside the separation area are presented in Fig.3. It is seen that this process is connected with the splitting up of the contact boundaries: the density is changing sharply but the value of pressure in the domain of splitting contact boundaries is close to constant. The turbulisation process is of pulsation character (as the flow in whole) and is caused by the cyclical generation of the reversal eddies in the separation area. The turbulization is taken place when the reversal eddies achieve the boundaries of the heated channel and interact with it. At that time the bow shock wave is allocated approximately in the nearest position to the body (Fig.3a, 3c). When the bow shock moves from the body the reversal eddies are absent and turbulent mixing becomes weaker (Fig.3b). After that the process is repeated. The fields of the flow velocities for turbulent mixing inside the separation area at two time moments are presented in Fig.4. It is seen that the process is accompanied by the new circulation flows generation.

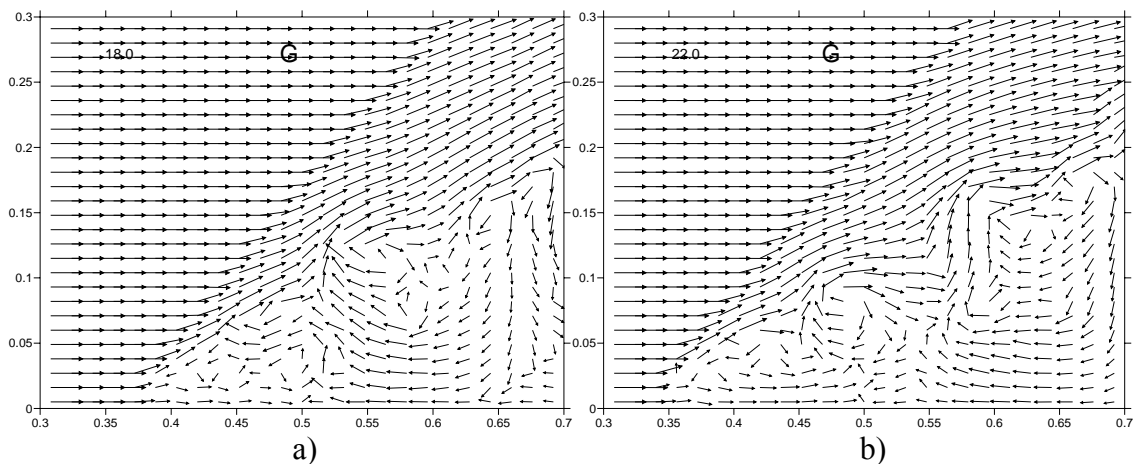


Fig.4. Velocity fields for the process of turbulent mixing inside the separation area, a) $t=18.0$, b) $t=22.0$.

In the case of $d=0.25$ the eddies are weaker and the processes of turbulent mixing is registered at the beginning of the interaction processes. On the contrary with the results for $d=0.1$ in this case the turbulent mixing is initiated by the vortices generated via shear-layer instability (Fig.5).

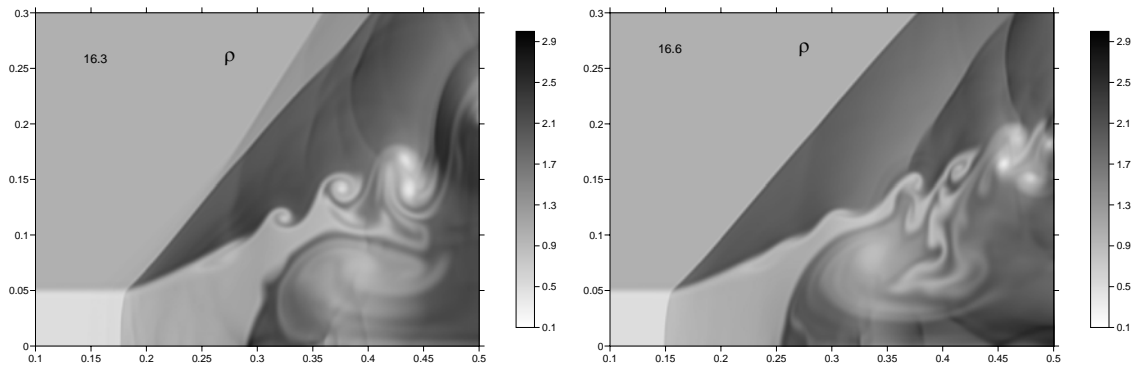


Fig.5. Fields of density, $d=0.25$: turbulent mixing inside the separation area at the beginning stage, a) $t=16.3$, b) $t=16.6$.

4. Dynamics of defining flow parameters.

Time history of the bow shock wave coordinate is presented in Fig.6. It is seen that the first pulsation is stronger for $d=0.1$ and the last pulsations are less significant. It is caused by the effect of the vortices generated via instabilities which are stronger than in the case of $d=0.25$. Thus, the vortices stabilize the bow shock wave to a certain degree.

History in time of the parameters in the stagnation point for $d=0.1$ and $d=0.25$ is presented in Fig.7. Eddies consisting of the twisted boundaries generate stochastically, move towards upper corner of the body and reflects from the body causing weak shock waves series towards the bow wave and a series of shock waves (and simple compression waves) normal to the front body's surface. Cumulating of these shock waves on the symmetry axis is the reason of stagnation pressure peaks arising and its pulsation accordingly with regard to compression waves¹¹.

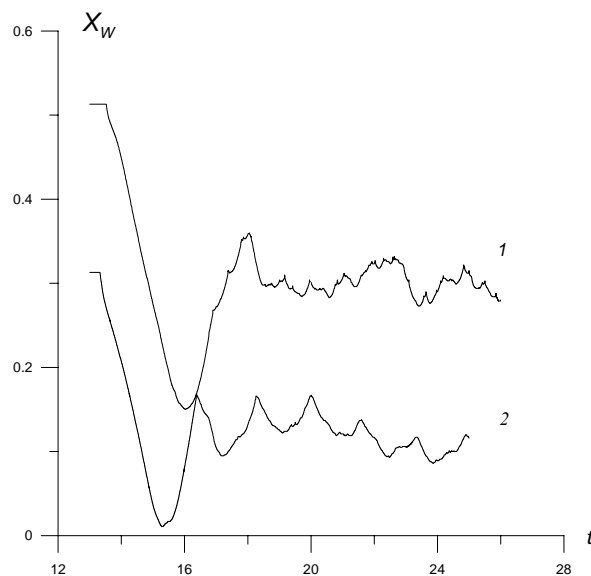


Fig.6. History in time of the bow shock wave coordinate, curve 1 – $d=0.1$, curve 2 – $d=0.25$.

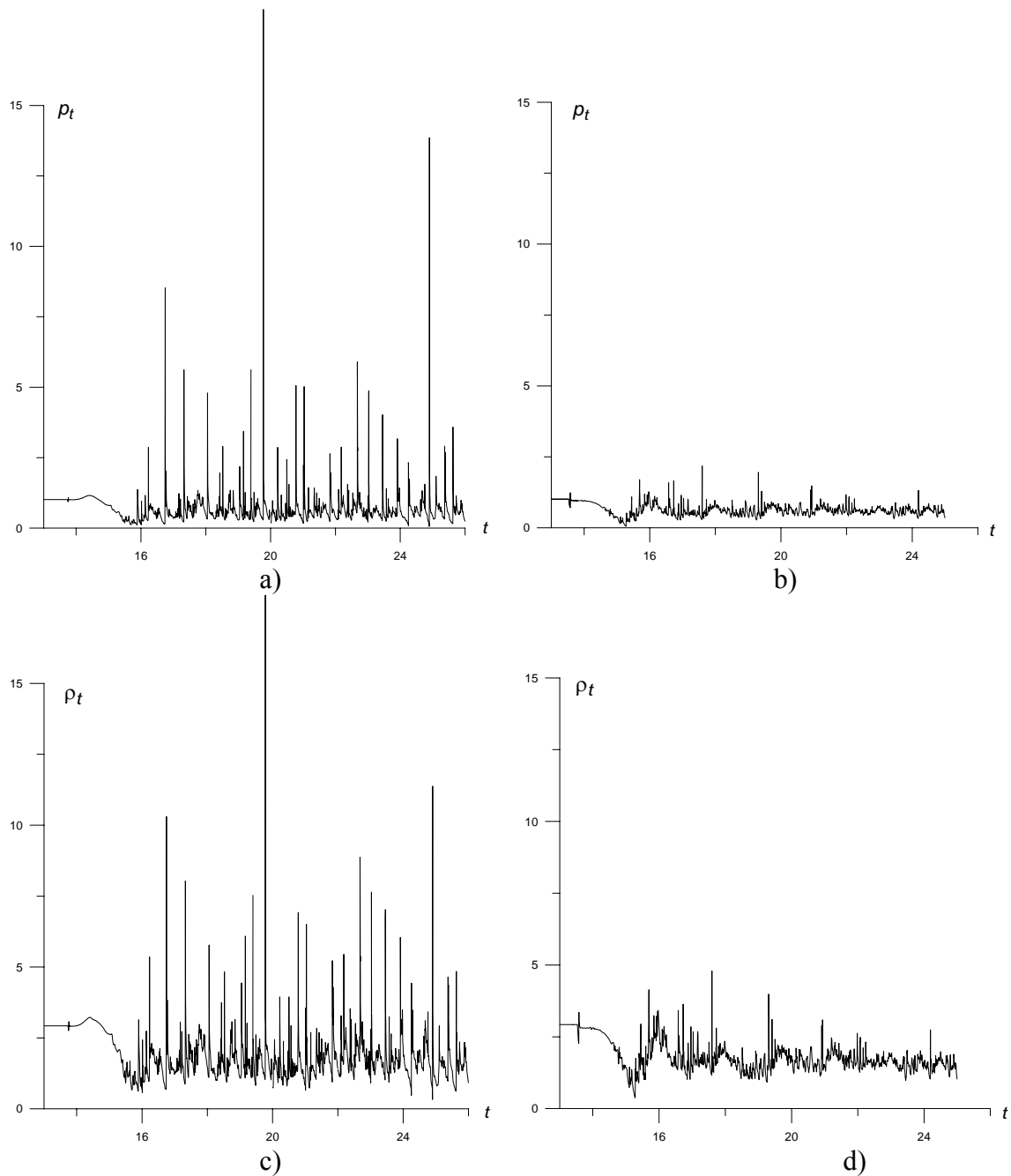


Fig.7. History in time of the parameters in the stagnation point, a) pressure, $d=0.1$, b) pressure, $d=0.25$, c) density, $d=0.1$, d) density, $d=0.25$.

The cumulating effects are more dramatically expressed for thin channels ($d=0.1$). Note, that the values of the attitudes of the peaks are not defined correctly both theoretically and numerically, numerical peaks may reach 10%-30%. It is seen that the process is the superposition of the large scaled pulsations and small scaled stochastic process. It should be emphasized that in the case of the thin channel the stochastic process dominates with the large scaled flow pulsations.

The last conclusion is clearly suggested by the time history of the front drag force. The dynamics of the front drag force (divided to 2π) F ,

$$F = \int_0^{R_b} pr dr ,$$

is presented in Fig.8. It is seen that the attitudes of stochastic fluctuations are greater to significant degree for thin channel ($d=0.1$) in comparison with the results for less thin channels ($d=0.25$).

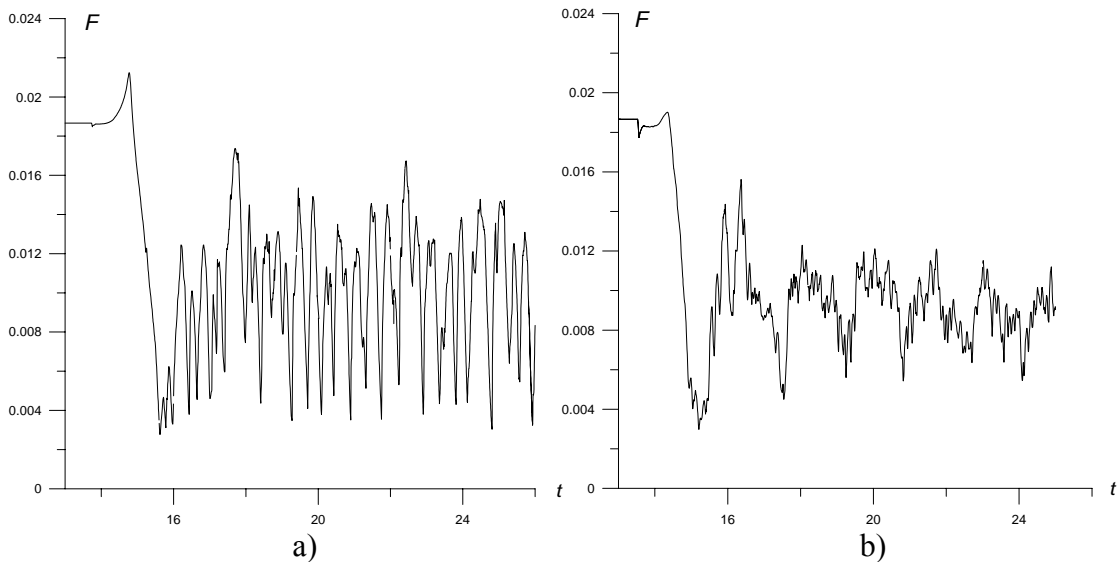


Fig.8. History in time of the front drag force, a) $d=0.1$, b) $d=0.25$.

CONCLUSIONS

Investigation of details of flow structure during the interaction of an infinite rarefied channel with cylinder shock layer is implemented for the value of the relation of the channel radius to the body's radius d equal to 0.1 and 0.25:

- stochastic pulsation flow mode is established;
- generation of contact discontinuity similar to Richtmayer-Meshkov instability and shear-layer instabilities have been obtained;
- flow dynamics parameters are characterized.

In the case of thin channel ($d=0.1$):

- formation of the heated channel inside the shock layer is established;
- the vortices generated via shear-layer instabilities are established to be stronger than for $d=0.25$;
- the reversal vortices are stronger, too, and as a result the process of turbulization of the separation area is more intensive;
- the reversal eddies generated were found to be strong sufficiently for the achievement of the turbulent mixing of the hot gas in the formed channel and cold surrounding gas inside the separation area;
- turbulent mixing is taken place cyclically in dependence with the flow phase when the eddies return to the separation area;
- it is shown that the small scaled stochastic process dominates with the large scaled flow pulsations.

In the case of less thin channel ($d=0.25$):

- the processes of turbulent mixing is registered at the beginning of the interaction processes and is initiated by the vortices generated via shear-layer instability;
- the processes of turbulent mixing via reversal eddies doesn't established.

REFERENCES

- [1] P.Y. Georgievskii, V.A. Levin. Supersonic flow over bodies in the presence of external energy Input // *Letters in Journal of Technical Physics*, 14, 8, 684-687 (1988).
- [2] V.I. Artem'ev, V.I. Bergel'son, I.V. Nemchinov, T.I. Orlova, V.A. Smirnov, V.M. Hazins. Changing the regime of supersonic streamlining obstacle via arising the thin channel of low density // *Mechanics of Liquids and Gases*, 5, 146-151 (1989).
- [3] A. Michalke. On spatially growing disturbances in an inviscid shear layer // *J. Fluid Mech.* 23, part 3, 521-544 (1965).
- [4] Meshkov E.E. Instability of a boundary between two gases accelerated by a shock wave // *Izv. An SSSR, MGG*, 5, 151-157 (1969).
- [5] G.L. Brown, A. Roshko. On density effects and large structure in turbulent mixing layers // *J. Fluid Mech.* 64, part 4, 775-816 (1974).
- [6] P.Y. Georgievskii, V.A. Levin. Stability problem for front separation regions control realized by energy deposition // *Paper AIAA*, 402, 1-7 (2006).
- [7] Yu. F. Kolesnichenko, V.G. Brovkin, O.A. Azarova, V.G. Grudnitsky et al. Microwave energy release regimes for drag reduction in supersonic flows // *Paper AIAA*, 353, 1-13 (2002).
- [8] O.A. Azarova, V.G. Grudnitsky, Yu. F. Kolesnichenko. Numerical Analysis of a Thin Low Density Channel Effect on Supersonic Flow past Bodies with Wedge-Shaped Ledges // *Mathematical Modeling*, 18, 10, 104-112 (2005).
- [9] O.A. Azarova, V.G. Grudnitsky, Yu. F. Kolesnichenko. Stationary streamlining bodies by supersonic flow with an infinite thin low density channel // *Mathematical Modeling*, 18, 1, 79-87 (2006).
- [10] Yu. F. Kolesnichenko, O.A. Azarova, V.G. Brovkin, D.V. Khmara et al. Basics in beamed MW energy deposition for flow/flight control // *Paper AIAA*, 669, 1-14 (2004).
- [11] O.A. Azarova, Yu. F. Kolesnichenko. On Details of Flow Structure during the Interaction of an Infinite Rarefied Channel with Cylinder Shock Layer // *Proc. of the 7th Int. Workshop on Magnetoplasma Aerodynamics, Moscow, 2007* (to be printed).
- [12] V.G. Grudnitsky, Yu. A. Prohorchuk. One approach to constructing difference schemes with arbitrary order of approximation of differential equations in partial derivatives // *Dokl. AN SSSR*, 234, 6, 1249-1252 (1977).